SEISMIC DESIGN AND ASSESSMENT OF SELF-CENTERING STEEL FRAMES WITH VISCOUS DAMPERS

Angelos S. Tzimas
Post-doctoral Research Fellow
School of Engineering, University of Warwick
Coventry, UK
E-mail: A.Tzimas@warwick.ac.uk

Athanasios D. Dimopoulos
PhD student
School of Engineering, University of Warwick
Coventry, UK
E-mail: A.Dimopoulos@warwick.ac.uk

Theodore L. Karavasilis
Associate Professor in Structural Engineering
School of Engineering, University of Warwick
Coventry, UK
Email: T.Karavasilis@warwick.ac.uk

1 ABSTRACT

This paper focuses on seismic design and assessment of steel self-centering moment-resisting frames (SC-MRFs) with viscous dampers within the framework of Eurocode 8 (EC8). Performance levels are defined with respect to drifts, residual drifts and limit states in the post-tensioned (PT) connections. A preliminary pushover analysis is conducted at the early phase of the design process to estimate rotations and axial forces in PT connections instead of using approximate formulae. Different designs of an SC-MRF with viscous dampers are considered to investigate all possible design scenarios. Nonlinear dynamic analyses confirm the minimal-damage performance of the SC-MRFs. It is shown that the use of the preliminary pushover analysis makes the design procedure very accurate in predicting structural limit states. Moreover, supplemental damping along with strict design criteria for the post-tensioned connections are found to significantly improve the seismic performance of the SC-MRFs.

2 INTRODUCTION

Conventional seismic resistant structures are designed to sustain significant inelastic deformations in main structural members under the design basis earthquake (DBE) [1]. Inelastic deformations result in damage and residual drifts, and so, in economic losses such

as repair costs and downtime. Steel self-centering moment-resisting frames (SC-MRFs) using post-tensioned (PT) beam-column connections are a promising class of resilient structures. SC-MRFs exhibit softening force-drift behaviour and eliminate beam inelastic deformations and residual drifts as the result of gap openings developed in beam-column interfaces and elastic PT bars which clamp beams to columns and provide self-centering capability. PT connections use energy dissipation devices which are activated when gaps open and can be easily replaced if damaged. Seismic design procedures for steel SC-MRFs have been proposed [2, 3] but research towards the standardization of SC-MRFs within the framework of Eurocode 8 (EC8) [1] is missing. Moreover, research on steel SC-MRFs equipped with viscous dampers with the goal of reducing drifts and controlling both structural and non-structural damage has not been conducted.

This paper focuses on seismic design and assessment of steel SC-MRFs with viscous dampers within the framework of EC8. Performance levels are defined with respect to drifts, residual drifts and limit states in the PT connections. A preliminary pushover analysis is conducted at the early phase of the design process to estimate rotations and axial forces in PT connections instead of using approximate formulae. Different designs of an SC-MRF with viscous dampers are considered to investigate all possible design scenarios. Nonlinear dynamic analyses confirm the minimal-damage performance of the SC-MRFs and the accuracy of the design procedure to predict the structural limit states.

3 STRUCTURAL DETAILS OF A PT CONNECTION WITH WHPS

Fig. 1(a) shows a SC-MRF using PT connections with web hourglass shape pins (WHPs) and Fig. 1(b) shows an exterior PT connection with WHPs. Two high strength steel bars, located at the mid depth of the beam, one at each side of the beam web, pass through holes drilled on the column flanges. The bars are post tensioned and anchored to the exterior columns. WHPs are inserted in aligned holes on the beam web and on supporting plates welded to the column flanges. Energy is dissipated through inelastic bending of the WHPs that have an optimized hourglass shape with enhanced fracture capacity [4]. The beam web and the beam flanges are reinforced with steel plates. The panel zone is strengthened with doubler and continuity plates. A fin plate welded on the column flange and bolted on the beam web is used for easy erection and resistance against gravity loads before post-tensioning. Slotted holes on the beam web ensure negligible influence of the fin plate on the PT connection behaviour. To avoid brittle failures in the PT connection due to beam web/flange inelastic buckling (seen in experiments and finite element analyses [5]), the use of a fuse-PT bar mechanism is adopted (similar in concept to the fuse system proposed in [6]). A short stocky steel beam (referred to as 'fuse') is welded on a strong plate bolted on the exterior column flange to enable replacement. PT bars are anchored on a stiff plate welded on the exterior face of the fuse. The fuse is designed to yield at a predefined force level to limit the peak force and elongation of the PT bars.

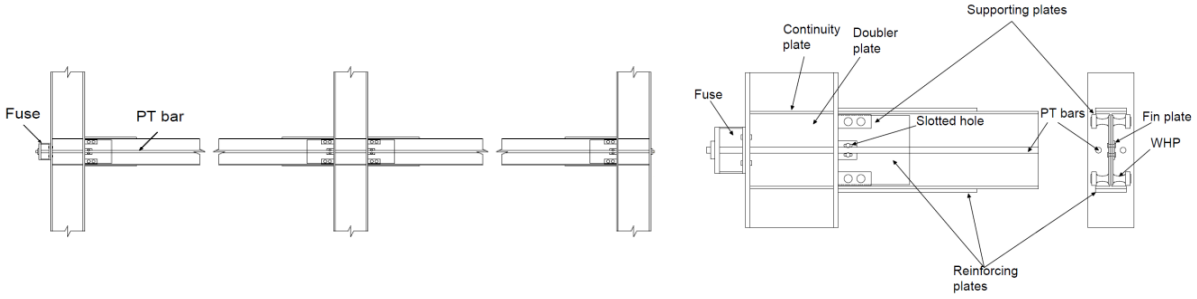

Fig. 1. a) SC-MRF; b) Exterior PT connection with WHPs

4 PT CONNECTION BEHAVIOR

Fig. 2(a) shows the free body diagram of an external PT connection where d_{1u} and d_{1l} are the distances of the upper and lower WHPs from the centre of rotation that is assumed to be at the inner edge of the beam flange reinforcing plates; d_2 is the distance of the PT bars from the center of rotation ; T is the total force in both PT bars; $F_{WHP,u}$ and $F_{WHP,l}$ are the forces in the upper and lower WHPs; C_F is the compressive force in the beam-column interface; V_{Ciu} and V_{Cil} are the shear forces in the upper and lower column, M is the PT connection moment, V is the beam shear force; and N is the horizontal clamping force in the beam-column interface. Fig. 2(b) shows the SC-MRF expansion due to rotations θ in the PT connections. F_{Dj} are the slab inertia forces transferred (by the secondary beams) to the mid-depth of all the beams j up to the point of the examined internal connection.

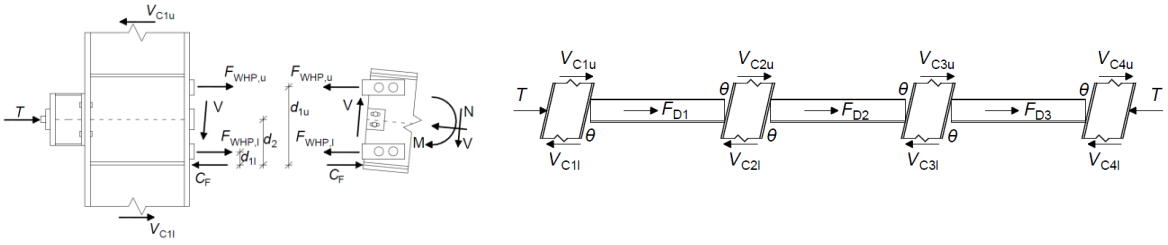

Fig. 2. a) Free body diagram of an external PT connection; b) SC-MRF expansion and horizontal forces of equilibrium

Fig. 3(a) shows the theoretical cyclic M-θ behaviour of the PT connection with WHPs. M is given by $M=M_N+M_{WHP}$, where M_N is the moment contribution from N (shown in Fig. 3(b)) and M_{WHP} is the moment contribution from the WHPs (shown in Fig. 3(c)). After decompression of the PT connection (Point 1 in Fig. 3(a)), gap opens and the behavior becomes nonlinear elastic with rotational stiffness S_1. At point 2, the upper WHPs yield and M continues to increase with slope S_2. At point 3, the lower WHPs yield and M continues to increase with slope S_3. At point 4, the fuse yields and M continues to increase with slope S_4. When loading is reversed, the connection begins to unload until the gap closes. Equations to calculate $S_{WHP,1}$ to $S_{WHP,3}$, $S_{N,1}$ to $S_{N,2}$, S_1 to S_4 and θ_2 to θ_4 are presented in [7].

The M_{WHP}-θ is multi-linear elastoplastic. The M_N-θ curve changes slope at θ_4 when the fuse yields. When the loading is reversed and until gap closes, the fuse unloads with its initial stiffness (without yielding in the opposite direction) and the PT bars with their elastic stiffness. Due to residual plastic shortening of the fuse the length of the PT bars is reduced, and so, their force when the gap closes is lower than the initial post-tensioning force.

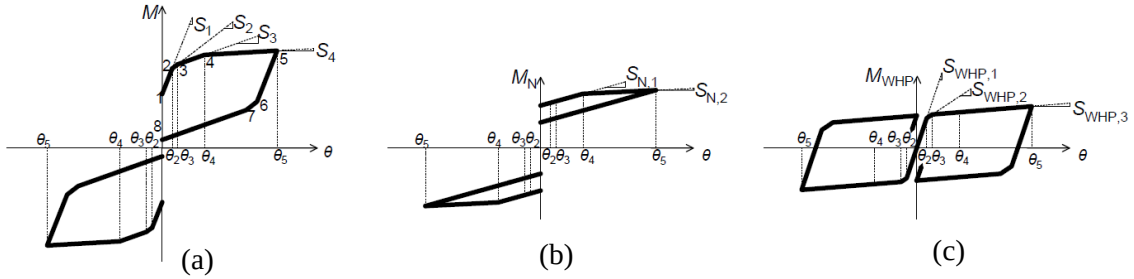

Fig. 3. Theoretical cyclic behaviour of the PT connection with WHPs

5 DESIGN PROCEDURE FOR PT CONNECTIONS WITH WHPS

Given the rotations of the PT connection under the DBE and MCE (i.e. θ_{DBE} and θ_{MCE}) and the corresponding forces V_{Ciu}, V_{Cil} and F_{Dj} from a preliminary pushover analysis of the SC-MRF discussed in [7], the design procedure involves sizing of the connection components (e.g. PT bars, WHPs, fuse, reinforcing plates) to achieve a target connection performance, and has the following steps: (1) calculation of the initial post-tensioning force; (2) design the PT bars and the fuse device; (3) design the WHPs; (4) self-centering capability checks; and (5) design the reinforcing and supporting frames. A complete methodology is presented in [7].

6 CONCEPT OF VISCOUS DAMPERS IN PARALLELTO SC-MRFS

Steel SC-MRFs avoid damage in beams and eliminate residual drifts under the DBE, but have peak drifts similar to those of conventional steel MRFs, and so, experience appreciable non-structural damage under the DBE. This paper presents a strategy of combining steel SC-MRFs with viscous dampers to achieve structural and non-structural damage reduction. A prototype building is designed as a SC-MRF with or without viscous dampers. Different designs of the SC-MRF with viscous dampers are considered to investigate all possible scenarios, i.e. use of dampers to achieve drifts significantly lower than the EC8 drift limit; to significantly reduce steel weight without exceeding the EC8 drift limit; or to reduce steel weight and achieve drifts lower than the EC8 drift limit

7 DESIGN CACES OF A 5-STOREY PROTOTYPE BUILDING

Fig. 4(a) shows the plan view of the 5-storey, 5-bay by 3-bay prototype building having two identical SC-MRFs in the ‘x’ plan direction. Viscous dampers are inserted in the interior gravity frames (with pin connections) that are coupled with the perimeter SC-MRFs through the floor diaphragm to form SC-MRFs with dampers as shown in Fig. 4(b). This paper focuses on one of the SC-MRFs with dampers, coupled through the floor diaphragm.

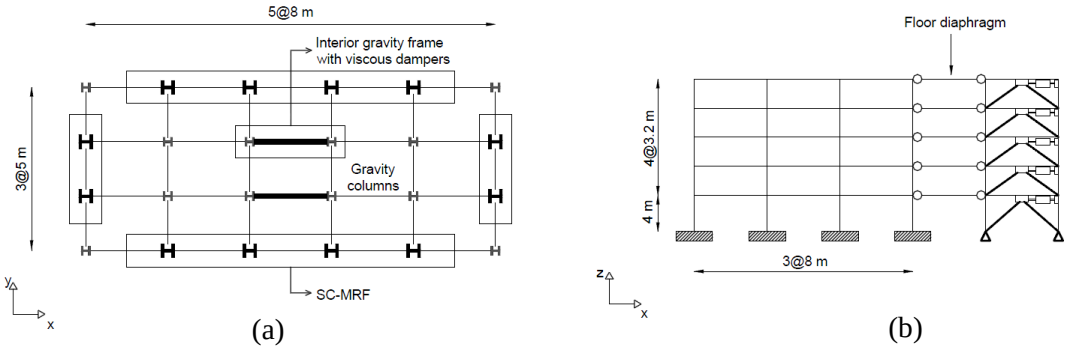

Fig. 4. (a) Plan view of the prototype building; (b) Elevation of the prototype building

Different versions of the SC-MRF with viscous dampers (Fig. 4(b)) are designed using the performance-based seismic design procedure presented in [7] to investigate different design scenarios. The PT connections of the SC-MRFs are designed for $M_{IGO}/M_{pl,b}$=0.65 and M_d/M_{IGO}=0.6, where M_{IGO} is the moment at point 2 in Fig. 3(a), $M_{pl,b}$ is the plastic moment of resistance of the beam and M_d is the moment contribution from the initial post-tensioning force in both PT bars [2-7]. To ensure structural and non-structural damage

harmonization, stricter design criteria (beam flange reinforcing plate length [2], γ_{PT} and θ_4) are adopted for the PT connections of the SC-MRFs designed for lower $\theta_{s\text{-}max}$. Table 1 provides a direct comparison of the steel weight, period *T*, total damping ratio ξ_t (equal to 3% for frames without dampers) and design criteria of the SC-MRFs which are discussed below.

CP3D100W: Conventional performance SC-MRF without viscous dampers (ξ_t =3%).

HP20D100W: High performance SC-MRF with viscous dampers (ξ_t =20%). Its target performance led to the same cross sections and PT connections details with those of CP3D100W. It demonstrates the design scenario where viscous dampers are used to achieve $\theta_{s,max}$ significantly lower than the EC8 limit. It also demonstrates the design scenario where strict design criteria for the PT connections along with a low $\theta_{s,max}$ target value are enforced to genuinely achieve seismic resilience.

CP11D86W: Conventional performance SC-MRF with viscous dampers (ξ_t =11%). Its steel weight is 86% the steel weight of CP3D100W. It represents the design scenario where viscous dampers are used to reduce steel weight without exceeding the EC8 $\theta_{s,max}$ limit.

HP19.5D86W: High performance SC-MRF with viscous dampers (ξ_t=19.5%). Its target performance led to the same cross sections and PT connections details with those of CP11D86W. It represents the design scenario where viscous dampers are used to reduce steel weight and achieve $\theta_{s,max}$ lower than the EC8 limit.

CP22D70W: Conventional performance SC-MRF with viscous dampers (ξ_t=22%). Its steel weight is 70% the steel weight of CP3D100W. It represents the design scenario where viscous dampers are used to significantly reduce steel weight without exceeding the EC8 $\theta_{s,max}$ limit.

8 MODELING IN OPENSEES

A nonlinear model for PT connections with WHPs has been developed in OpenSees. In this model the PT connections and the associated beams and columns, consist of nonlinear beam-column elements, and hysteretic and contact zero-length spring elements, appropriately placed in the beam-column interface. A detailed description of this model can be found in [7].

SC-MRF	Steel Weight (kN)	*T* (s.)	ξ_t (%)	$\theta_{s,max}$ FOE (%)	$\theta_{s,max}$ DBE (%)	$\theta_{s,max}$ MCE (%)	γ_{PT} *	θ_4 fuse activation
CP3D100W	268	1.27	3.00	0.72	1.80	2.70	2.1	θ_{DBE}
HP20D100W	268	1.27	20.0	0.48	1.20	1.80	3.5	$1.5\theta_{DBE}$
CP11D86W	230	1.63	11.0	0.72	1.80	2.70	2.1	θ_{DBE}
HP19.5D86W	230	1.63	19.5	0.60	1.50	2.25	2.6	$1.2\theta_{DBE}$
CP22D70W	190	2.22	22.0	0.72	1.80	2.70	2.1	θ_{DBE}

* Safety factor against PT bar yielding

Table 1. Design properties of the SC-MRFs

9 SEISMIC EVALUATION

9.1 *Pushover analyses*

Monotonic pushover analyses up to 10% roof drift (θ_r) and cyclic pushover analyses up to the DBE θ_r for all five design cases have been performed. Supplemental damping results in

lower drifts under the same seismic intensities, and so, in higher structural and non-structural performance. Due to space limitation, Fig. 5 shows only the results of the HP20D100W and CP3D100W frame. As shown in Fig. 5 HP20D100W frame eliminates residual drifts under the DBE compared to CP3D100W frame.

The development of column plastic hinges in lighter SC-MRFs occurs at drifts higher than those in heavier SC-MRFs, and so, residual drifts in lighter SC-MRFs are reduced. The descending branch of the pushover curve denotes static collapse of the structure and initiates at θ_r higher than 5% due to beam local buckling in all SC-MRFs apart from the CP22D70W that experiences negative static stiffness solely due to excessive P-Δ effects.

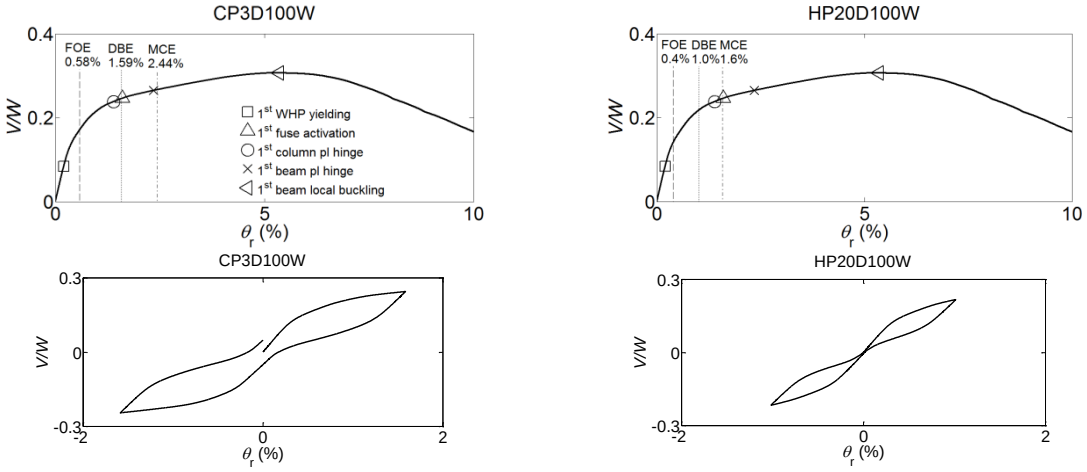

Fig. 5. Monotonic and cyclic pushover curves of CP3D100W and HP20D100W

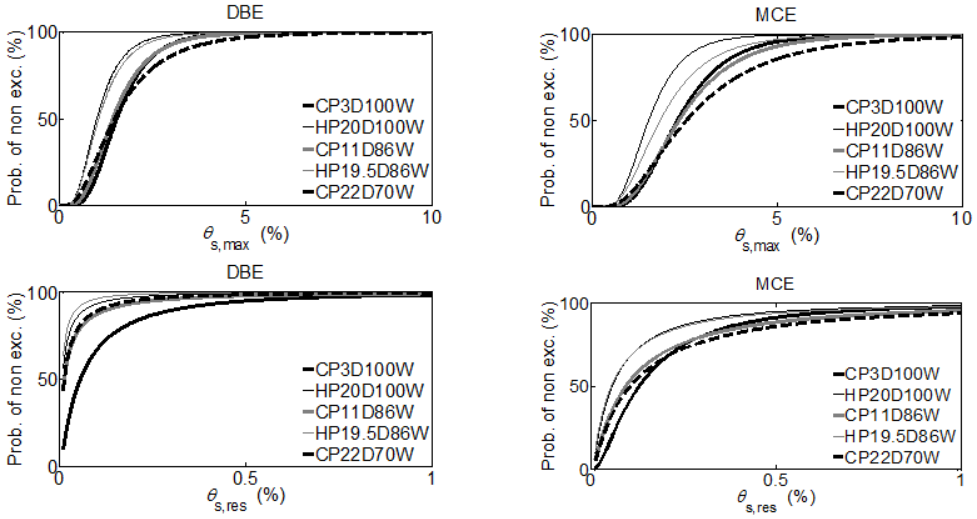

Fig. 6. Fragility curves of $\theta_{s,res}$ and $\theta_{s,max}$ under DBE and MCE

9.2 *Fragility curves*

Dynamic nonlinear analyses have been conducted to evaluate the seismic performance of all design cases. The ground motions were scaled to the DBE and MCE. Having the peak storey drifts ($\theta_{s,max}$) and residual drifts ($\theta_{s,res}$) for all the SC-MRFs after the dynamic analyses, fragility curves are constructed. Fig. 6 shows the $\theta_{s,max}$ and $\theta_{s,res}$ fragility curves

of the SC-MRFs under the DBE and MCE. High performance SC-MRFs have significantly better performance with $\theta_{s,max}$ and $\theta_{s,res}$ fragility curves clearly shifted to the left. This demonstrates the effectiveness of supplemental damping to improve the structural and non-structural performance of SC-MRFs. All conventional performance SC-MRFs have almost identical performance, apart from probabilities of non-exceedance higher than 70% under the DBE and 50% under the MCE for which CP22D70W has a worse performance. This demonstrates that steel SC-MRFs with viscous dampers can be designed for less steel weight without compromising their seismic performance. However, a limit on the strength reduction may need to be established. None of the SC-MRFs becomes globally unstable under the MCE.

10 CONCLUSIONS

A prototype building was designed as an SC-MRF with or without viscous dampers. SC-MRFs with different base shear strength and supplemental damping were investigated. Pushover and seismic analyses were conducted in OpenSees using models capable to capture all structural limit states up to collapse. Analyses results confirm the minimal-damage performance of the SC-MRFs. It is shown that the use of the preliminary pushover analysis makes the design procedure very accurate in predicting structural limit states. Moreover, supplemental damping along with strict design criteria for the post-tensioned connections are found to significantly improve the seismic performance of the SC-MRFs.

ACKNOWLEDGEMENTS

Financial support for this work is provided by the Engineering and Physical Sciences Research Council of the United Kingdom; Grant Ref: EP/K006118/1.

REFERENCES

[1] EUROCODE 8. Design of structures for earthquake resistance. 2004.

[2] GARLOCK M., SAUSE R. and RICLES J.M. "Behaviour and design of posttensioned steel frame systems". *Journal of Structural Engineering, ASCE,* Vol. 133, No 3, 2007, pp. 389-399.

[3] KIM H.J. and CHRISTOPOULOS C. "Seismic design procedure and seismic response of post-tensioned self-centering steel frames". *Earthquake Engineering and Structural Dynamics, Vol.* 38, 2009, pp. 355-376.

[4] VASDRAVELLIS G., KARAVASILIS T.L. and UY B. "Large-scale experimental validation of steel post-tensioned connections with web hourglass pins". *Journal of Structural Engineering, Vol.* 139, 2013, pp. 1033-1042.

[5] VASDRAVELLIS G., KARAVASILIS T.L. and UY B. "Finite element models and cyclic behaviour of self-centering post-tensioned connections with web hourglass pins". *Engineering Structures, Vol.* 52, 2013, pp. 1-16.

[6] LIN YC, SAUSE R, RICLES JM. Seismic performance of a large-scale steel self-centering moment resisting frame: MCE hybrid simulations and quasi-static pushover tests. *Journal of Structural Engineering,* Vol.139, No. 7, 2013, pp. 1227-1236.

[7] TZIMAS A.S., DIMOPOULOS A.I and KARAVASILIS T.L. "EC8-based seismic design and assessment of self-centering steel frames with viscous dampers". *Journal of Constructional Steel Research,* 2014, Under review.

ΑΝΤΙΣΕΙΣΜΙΚΟΣ ΣΧΕΔΙΑΣΜΟΣ ΚΑΙ ΑΠΟΤΙΜΗΣΗ ΜΕΤΑΛΛΙΚΩΝ ΠΛΑΙΣΙΩΝ ΜΕ ΑΥΤΟ-ΕΠΑΝΑΦΕΡΟΜΕΝΕΣ ΣΥΝΔΕΣΕΙΣ ΚΑΙ ΙΞΩΔΕΙΣ ΑΠΟΣΒΕΣΤΗΡΕΣ

Άγγελος Σ. Τζίμας
Μετα-διδακτορικός ερευνητής
School of Engineering, University of Warwick
Coventry, UK
E-mail: A.Tzimas@warwick.ac.uk

Αθανάσιος Δ. Δημόπουλος
Διδακτορικός φοιτητής
School of Engineering, University of Warwick
Coventry, UK
E-mail: A.Dimopoulos@warwick.ac.uk

Θεόδωρος Λ. Καραβασίλης
Αναπληρωτής καθηγητής
School of Engineering, University of Warwick
Coventry, UK
Email: T.Karavasilis@warwick.ac.uk

ΠΕΡΙΛΗΨΗ

Τα μεταλλικά πλαίσια με συνδέσεις που έχουν την ικανότητα να επανέρχονται στην αρχική τους θέση ελαχιστοποιούν τη βλάβη στις δοκούς και τις παραμένουσες μετατοπίσεις του κτιρίου. Στην παρούσα εργασία εξετάζεται ο αντισεισμικός σχεδιασμός μεταλλικών πλαισίων με αυτο-επαναφερόμενες συνδέσεις και ιξώδεις αποσβεστήρες, στα πλαίσια του EC8, με στόχο την ελαχιστοποίηση της βλάβης των δομικών και μη δομικών στοιχείων. Τα επίπεδα επιτελεστικότητας των πλαισίων ορίζονται με βάση τις επιτρεπόμενες σχετικές μετατοπίσεις, παραμένουσες μετατοπίσεις και τα επίπεδα βλάβης των αυτο-επαναφερόμενων συνδέσεων. Εξετάζονται διαφορετικά σενάρια σχεδιασμού ενός πενταώροφου κτιρίου. Τα αποτελέσματα στατικών και δυναμικών μη γραμμικών αναλύσεων δείχνουν την αξιοπιστία της μεθοδολογίας αντισεισμικού σχεδιασμού καθώς και τα σημαντικά πλεονεκτήματα των πλαισίων με αυτο-επαναφερόμενες συνδέσεις και ιξώδεις αποσβεστήρες έναντι των συμβατικών αντισεισμικών μεταλλικών πλαισίων.